Electrochemical detection of nitrite and ascorbic acid at glassy carbon electrodes modified with carbon nano-onions bearing electroactive moieties

Joanne P. Bartolome, Alex Fragoso*

Nanobiotechnology & Bioanalysis Group, Departament d'Enginyeria Química, Universitat Rovira i Virgili, Avinguda Països Catalans 26, 43007 Tarragona, Spain.

E-mail: alex.fragoso@urv.cat

Abstract

In this work, we evaluate two novel surfaces for the simultaneous detection of nitrite and ascorbic acid in aqueous media. Glassy carbon electrodes were first modified with small carbon nano-onions (GCE/CNO) and further functionalized either by electrografting ortho-aminophenol (*o*AP) groups or by physical adsorption of thionine to give electroactive surfaces that were characterized by cyclic voltammetry. The modified surfaces exhibited a fast electrochemical response and were able to detect the presence of nitrite and ascorbic acid by amperometry. The presence of both CNOs and the electroactive moiety on the electrode surface enhanced the sensitivity and lowered the limit of detection of the determinations as compared to GCE modified only with *o*AP or thionine. The CNO-modified electrodes showed good reproducibility and stability with time and were applied in the detection of ascorbic acid in orange juice.

1. Introduction

Nitrite and ascorbic acid (AA) are two of the most widely used additive compounds in products for human consumption. They are controlled substances and thus there is an increasing interest in their analysis [1-5]. Ascorbic acid has been recognized as an important food stabilizer to improve nutritional value and prevent autooxidation of products [6,7]. Although ascorbic acid toxicity is very rare, a high dose can lead to stomach upset and diarrhea [8]. On the other hand, nitrite is a useful preservative in food industry to enhance color and extend the shelf life of processed meats. However, nitrite ions can react with amines to form nitrosamines, which are well known carcinogenic substances [9,10] (Scheme 1).

Various methods have been proposed for the detection of AA and nitrite such as chromatography [11-13], spectroscopic techniques [14-16] and electrochemical analysis [17-23]. However, these molecules can be directly oxidized in the surface of conventional electrodes at relatively high overpotentials. Many new materials have been suggested to overcome this problem. In particular, carbon nanomaterials such as nanotubes, graphene or mesoporous carbon have gained a lot of interest in bioanalysis due to a combination of large surface area, good electrical conductivity and ease of functionalization [24]. These properties have made them good candidates to develop nitrite and ascorbic acid sensors [25-32]. Zhu et al. [31], prepared modified poly(amidoamine) dendrimer carbon nanotubes for the determination of nitrite held at +0.73 V as oxidation potential using chronoamperometry. Nanodiamond powder electrodes for the analysis of nitrite was investigated by Chen et al. [32] in which the oxidation of nitrite appears around +1.05 V using cyclic voltammetry (CV) and differential pulse voltammetry (DPV). The oxidation of ascorbic acid on ZnO-decorated reduced graphene oxide electrode was observed at around +0.2 V [26] while

poly(xanthurenic acid)/multiwalled carbon nanotube (MWCNT) modified electrodes were used for the amperometric determination of ascorbic acid at +0.3 V [25a].

Scheme 1

Carbon nano-onions (CNOs) are multi-layered fullerenes concentrically arranged one inside the other and were first reported by Ugarte in 1992 after irradiating a sample of carbon soot particles under an electron beam [33]. Their average sizes typically range from 5 nm to 40 nm in diameter and, unlike other carbon allotropes, they remain relatively less explored [34]. Recently, CNOs have been reported as attractive candidates for the development of electrochemical detection systems due to their morphological and electrical properties since they can significantly increase the electroactive surface when deposited on electrode surfaces and enhance electron transfer [35]. To the best of our knowledge, there is only one example of application of CNOs in electrochemical detection of small molecules [36]. A mixture of carbon CNO/poly(diallyldimethylammonium chloride)-composites were deposited on a gold electrode then the electrochemical properties of the surface were tested for the ability to detect dopamine in the presence of uric and ascorbic acid. Their findings showed good selectivity and sensitivity of the modified electrodes.

Diazonium salts ($R\text{-}N{\equiv}N^{+}\ X^{-}$) are a class of organic compounds prepared by the treatment of aromatic amines with sodium nitrite in the presence of a mineral acid. Their electrochemical reduction for covalent modification of conductive surfaces was first investigated by Pinson using isolated tetrafluoroborate salts [37] and further extended to *in situ* generated diazonium cations [38]. This method can be applied to a wide variety of surfaces such as carbon (including nanotubes and diamond), metals and metal oxides and provide an easy and

efficient way to covalently modify the surface of these materials [39,40]. In our group, we have exploited this technique to construct electrochemical sensors for ascorbic and uric acid based on *ortho*-aminophenol (*o*AP) films on glassy carbon surfaces [41-43].

Conversely, thionine (TH) is a thiazine derived aromatic dye containing two amino groups and generally used for dyeing. Thionine is also an electrochemical redox indicator being colorless in reduced form and violet when oxidized. Several studies have been conducted, particularly on carbon nanotubes, in which thionine was directly absorbed and attached to the surface creating a strong supramolecular π-π interaction [28,44-47]

Here we explore the combination of interfacial and electrochemical properties of CNOs with immobilized electroactive moieties on glassy carbon electrodes to build sensitive sensors for the detection of AA and nitrite.

2. Experimental

2.1 Reagents and instrumentation

The CNO sample used in this work was kindly provided by Dr. Luis Echegoyen (Department of Chemistry, University of Texas at El Paso). Dimethylformamide (DMF), L-ascorbic acid, 2-nitro-4-aminophenol, $NaNO_2$ and thionine were obtained from Sigma-Aldrich and used as received. All other chemicals used in buffer solutions preparation were of analytical-reagent grade. All solutions were prepared with Milli-Q water.

A tip sonicator (Ultraschall Processor UP200S) was used to mechanically disperse CNOs in 10 mL DMF. The modified electrodes were characterized by Environmental Scanning Electron Microscopy (ESEM) on a Quanta 600 microscope (FEI Company Inc.) under high vacuum at 25 kV. All electrochemical measurements were carried out using an Autolab model PGSTAT 12 potentiostat/galvanostat controlled with the general purpose

electrochemical system (GPES) software (Eco Chemie, The Netherlands), equipped with BASi C-3 Stand (RF-1085) three-electrode cell. This configuration contains a bare or chemically modified glassy carbon electrode (BAS model MF-2012, 3.0 mm diameter) as working electrode, a platinum wire as counter electrode and an Ag/AgCl(sat) as reference electrode. All potentials were recorded with respect to this electrode. Oxygen-free nitrogen was used to remove oxygen from the solutions and a continuous flow of nitrogen was maintained during the voltammetric measurements.

2.2 Electrochemical grafting of *o*AP on GCE/CNO

GCE/CNO electrodes were prepared was previously reported [35]. 2-nitro-4-aminophenyl films on GCE/CNO were prepared using essentially the same method as described before [43] with slight modifications. A cold mixture of 2-nitro-4-aminophenol (10 mM) and $NaNO_2$ (10 mM) was treated with 0.5 M HCl (degassed with N_2) for 10 min in an electrochemical cell. GCE/CNO electrodes were immersed and the potential was cycled from 0 V to -0.6 V at 100 mV/s for 60 scan cycles. The generated 2-nitrophenol film was rinsed and sonicated in Milli-Q water and electroreduced by applying 5 potential scans between 0 and -0.8 V at 100 mV/s in 0.1 M H_2SO_4. The electrodes were washed with Milli-Q water then subsequently subjected to potential scanning between -0.1 and 0.6 V for 10 cycles at 100 mV/s in phosphate buffer (0.1 M, pH 7.4) to remove the physically adsorbed compounds. The characterization of the film in the GCE/CNO/*o*AP electrodes was carried out by cyclic voltammetry between -0.4 to 0.6 V at different scan rates in phosphate citrate buffer pH 3.5. The same procedure was done with bare GCE that served as a control.

2.3 Preparation of thionine modified GCE/CNO electrode

GCE/CNO electrodes were immersed in a thionine solution (2 mg/mL) for several hours, then washed thoroughly with phosphate citrate buffer pH 3.5 with stirring to remove the

unbound thionine molecules. The modified GCE/CNO/TH were then subjected to 5 potential cycles between 0.6 V and -0.3 V at 100 mV/s in phosphate citrate buffer pH 3.5 in order to stabilize the thionine film [46]. The same procedure was performed with a bare GCE that served as a control.

2.4 Detection of nitrite and AA with GCE/CNO/*o*AP and GCE/CNO/TH electrodes

Amperometric measurements were carried out at +0.75 V or +0.20 V for the detection of nitrite and ascorbic acid, respectively, in an electrochemical cell containing 5 mL phosphate citrate buffer pH 3.5. The background current was measured under stirring conditions at 350 rpm. Subsequently, successive 50 µL aliquots of 1 mM nitrite or ascorbic acid were added to the cell and the current response was continuously recorded. Control experiments were carried out on GCE/*o*AP or GCE/thionine electrodes under the same conditions for comparison.

Intra-sensor (same sensor, different samples) and inter-sensor (same sample, different sensors) repeatability studies were conducted on GCE/CNO/*o*AP electrodes either by measuring the current obtained with five freshly prepared 10 µM samples of nitrite and AA on the same electrode (intra-sensor) or on five different sensors on one of the above samples (inter-sensor).

2.5 Reproducibility and stability studies

For the stability study, two batches of three GCE/CNO/*o*AP and GCE/CNO/thionine electrodes were fabricated and the current corresponding to 10 µM AA was measured and taken as the initial signal (100%). The sensors were stored in vacuo in dried conditions in the fridge and the current corresponding to 10 µM AA was measured in intervals of one week and divided by the initial value to construct a %initial signal *vs*. time plot.

2.6 Detection of AA in orange juice

A commercial orange juice sample (Hacendado), having a nominal amount of AA of 40 mg/100 mL was treated as described before [22]. An aliquot of the sample was diluted 1:1000 in phosphate citrate buffer pH 3.5 and measured as indicated above. The current value was interpolated in the calibration curve to determine the AA contents of the sample that was compared with the value obtained spectrophotometrically [22]. The measurements were carried out in triplicate.

3. Results and discussion

3.1 Electrochemical characterization of GCE/CNO/oAP electrodes

CNOs were deposited on GCE as reported earlier [35]. The GCE/CNO/*o*AP modified electrodes were prepared in two steps by electrografting the *in situ* prepared diazonium salt of 2-nitro-4-aminophenol followed by potential reduction of the resulting 2-nitro-phenol film in acidic medium (Scheme 2). Both functionalization steps were carried out using cyclic voltammetry by sweeping the potential cathodically until the corresponding reduction peaks appeared at -0.21 V and -0.55 V, respectively (Figure 1).

Scheme 2

Figure 1

The cyclic voltammograms of GCE/CNO/*o*AP modified electrodes at different scan rates showed the typical quasi-reversible signal associated with the oxidation and reduction of electrografted *oAP* at $E_{1/2}$ = -3 mV vs Ag/AgCl (Figure 2). The voltammetric response of GCE/CNO/*o*AP electrodes present much higher current intensities than the corresponding GCE/*o*AP prepared in a similar way although the $E_{1/2}$ is essentially the same. This

enhancement in the current signal is due to the increased surface area provided by the deposited CNOs [35].

Figure 2

The surface coverage of *o*AP in the surface of GCE/CNO/*o*AP was evaluated from the equation $\Gamma = Q/nFA$, where Q is the charge associated with the *o*AP oxidation peak (area under the curve corrected for the baseline) at a low scan rate (10 mV s^{-1}), n is the number of exchanged electrons (n = 2), F is the Faraday's constant and A is the area of the electrode calculated using the Randles-Sevcik equation on GCE/CNO. The calculated value of Γ was 2.71×10^{-9} mol cm^{-2}, which is about 3 times higher than that obtained for the grafting of *o*AP on GCE (0.93×10^{-9} mol cm^{-2}).

3.2 Electrochemical characterization of GCE/CNO/thionine electrodes

Thionine was immobilized on GCE/CNO electrodes by spontaneous adsorption (Scheme 3). The adsorption of thionine was studied as a function of time by cyclic voltammetry on both surfaces (Figure 3a-c). As can be seen, the redox signals of thionine increase with time with time and remain essentially constant after three hours on the GCE/CNO surface. This time was thus used in further experiments. In the case of GCE, the saturation is achieved after two hours, the redox response is markedly lower and gradually disappears with washing, indicating a weak interaction of thionine with the bare surface.

Scheme 3

Figure 3

Figure 3d shows the cyclic voltammograms of thionine modified GCE/CNO surface at different scan rates. The voltammetric response of thionine is characterized by broad successive peaks in both anodic and cathodic scans, indicating the electrochemical activity

of adsorbed thionine [46]. The current responses showed a linear relationship with scan rate, indicating surface confinement of thionine. After continuous potential cycling, the electrochemical characteristics of thionine were stable, indicating a strong interaction with the CNO surface. The surface coverage of thionine in the surface of GCE/CNO was 2.11×10^{-10} mol cm^{-2}. This surface coverage is about 6 times higher than that observed for GCE/thionine and essentially the same as that observed on GCEs modified with MWCNT [46]. Considering the dimensions of thionine (~58 $Å^2$) and assuming a planar stacking on the CNO surface, the theoretical coverage of thionine on GCE/CNO would be 2.77×10^{-10} mol cm^{-2} and therefore about 76% of the surface is actually covered. This is not surprising, considering the roughness of the CNO-modified surface that could hinder the formation of a perfectly adsorbed monolayer.

3.3 Electrochemistry of nitrite and ascorbic acid at GCE and GCE/CNO

The electrochemical response of AA and nitrite at GCE is characterized by irreversible anodic signals at 0.21 and 0.90 V (Figure 4a). Interestingly, at GCE/CNO electrodes both oxidation processes are favored and shifted to less positive potentials (0.09 and 0.80 V for AA and nitrite). Thus, the overpotential for the oxidation of nitrite is reduced by 110 mV (Figure 4b), indicating that the layer of CNOs favors the electron transfer reaction of nitrite, as observed previously [35]. This potential shifts are accompanied by an increase in the signal intensity due to the increased electrode area provided by the presence of the CNO layer.

Figure 4

3.4 Electrochemical detection of nitrite and ascorbic acid at GCE/CNO/*o*AP electrode

In order to evaluate the electrocatalytic activity of modified GCE/CNO/*o*AP surface towards the oxidation of AA and nitrite, cyclic voltammograms were recorded in phosphate citrate buffer pH 3.5 in the absence and presence of nitrite and ascorbic acid (Figure 4c). Upon the addition of nitrite on modified GCE/CNO/*o*AP, there is an irreversible oxidation peak at 0.78 V which corresponds to the two-electron oxidation process of NO_2^- to NO_3^- (Scheme 1). This peak potential is negatively shifted ~20 mV with respect to GCE/*o*AP indicating that the presence of CNO reduced the overpotential due to electronic effects of the graphitic onion layers [35] and also enhances the oxidation current due to an increase in surface area.

In the presence of AA, the CV response features a relatively broad anodic signal around 0.2 V, accompanied by a further signal increase with respect to the GCE/CNO electrode and a disappearance of the cathodic *o*AP peak. The enhancement in the anodic current close to the formal potential of the aminophenol/quinoneimine couple and the disappearance of the cathodic *o*AP peak suggest an electrocatalytic effect of the electroactive *o*AP film on the oxidation of AA. Interestingly, the peak maximum is now shifted ~40 mV to more positive values, which may be ascribed to the presence of the *o*AP film.

This surface was then used to detect ascorbic acid and nitrite by amperometric measurements at different potentials using the GCE/CNO/*o*AP electrode (Table 1). The amperometric measurements were done with either the presence of nitrite or ascorbic acid added into the buffer solution prior to the addition of the other analyte in order to assess if the presence of the other analyte in solution would somehow affect the current response. As can be seen in Figure 5a and 5b, the current responses rapidly achieved a steady current with the successive additions of 10 μM of each analyte indicating a fast electrochemical response.

Figure 5

A linear relationship of the current responses with the concentration of nitrite and AA was observed over the ranges of 0-50 μM (Figure 5c,d). The sensitivity for the detection of nitrite at GCE/CNO/*o*AP was 0.034 μA/μM with a correlation coefficient of 0.99. This value is almost 3 times more sensitive than GCE/*o*AP. The estimated limit of detection (LOD) of nitrite at GCE/CNO/*o*AP as obtained from the calibration curve was 0.82 μM which is 2 times lower as compared to GCE/*o*AP. For the detection of AA the sensitivity of the electrode is 0.024 μA/μM and the LOD was 0.34 μM. Compared with the reported GCE/*o*AP surface [41], the GCE/CNO/*o*AP sensor shows two times higher sensitivity and a more extended linear range than GCE/*o*AP. The obtained LOD is also lower than that reported for a spectrophotometric method. Hence, the incorporation of CNOs con the electrode surface resulted in better analytical performances as compared with *o*AP films electrografted on both, glassy carbon and screen-printed surfaces (Table 1).

3.5 Electrochemical detection of nitrite and ascorbic acid at GCE/CNO/thionine electrode

Figure 6 shows the cyclic voltammograms of GCE/CNO/thionine modified electrodes with the absence and presence of 100 μM nitrite and/or 100 μM AA in phosphate citrate buffer pH 3.5. Similarly to the *o*AP modified electrodes, upon addition of both analytes, the corresponding anodic signals appear in the voltammograms although the background signal corresponding to adsorbed thionine is higher. In the presence of AA the cathodic signal of thionine markedly decreased, indicating that the adsorbed dye effectively mediates in the electrocatalytic oxidation of AA, similarly to what has been observed for NADH on thionine/SWCNT electrodes [47].

Figure 6

Figure 7 shows the amperometric current responses and calibration curves in the modified GCE/CNO/thionine and GCE/thionine. In this case, the sensitivity for the detection of nitrite was 0.045 μA/μM (2 times more sensitive than GCE/thionine) with a LOD of 1.89 μM (6 times lower LOD than GCE/thionine). For the determination of AA the sensitivity was 0.043 μA/μM (9 times higher than GCE/thionine) and the LOD was 0.66 μM (2 times lower than GCE/thionine). The limit of detection for nitrite is comparable with that obtained with a spectrophotometric method based on the Griess reaction but shows a much longer linear range (Table 1).

Figure 7

3.6 Reproducibility and stability studies

To study the repeatability of the sensors, the electrochemical measurements were repeated with five 10 μM samples of nitrite and ascorbic acid on the same electrode. The relative standard deviation of the current responses for GCE/CNO/*o*AP with nitrite was 3.2% and 3.9% for ascorbic acid (Figure 8a). For GCE/CNO/thionine, the values were 2.8% for nitrite and 4.1% for ascorbic acid.

For GCE/CNO/*o*AP, the measurements were also carried out on the same sample but using five different electrodes. In this case, the relative standard deviation of the current responses was 6.1% for ascorbic acid and 5.1% for nitrite (Figure 8b). These low relative deviations derived from the responses indicate that the modified surfaces have an excellent operational reproducibility.

Both batches of GCE/CNO/*o*AP and GCE/CNO/thionine electrodes were found to be very stable, retaining up to 87% of the initial response observed for 10 μM of AA after 6 weeks when stored in dried conditions at 4^0C (Figure 8c).

Figure 8

3.7 Real samples and selectivity analysis in AA determination

To test the selectivity of the sensor, the effect of two potentially interfering substances present in fruits and juice samples was investigated. In both cases the signal recovery was very close to 100%, indicating that the tested sensors are selective and specific for the detection of AA (Table 2).

The applicability of the developed sensors in real samples was also studied by measuring the AA content of an orange juice sample using the GCE/CNO/*o*AP sensor (Table 3) and compared the results with a reported spectrophotometric method [22]. The good correspondence between both methods indicates that the sensor is able to work in real samples. A recovery of 104% of the theoretical signal was obtained after adding a standard solution of 10 μM AA to the sample.

Table 2

Table 3

Conclusions

Carbon nano-onions (CNOs) were used to modify glassy carbon electrodes followed either by electrochemical grafting of *ortho*-aminophenol or by physical adsorption of thionine. These electrodes were used for the simultaneously detection of nitrite and ascorbic acid in

aqueous solution at acidic pH. Remarkably, the presence of both CNO and the electroactive moiety provoked an enhancement in the sensitivity of the determination and lowered the limits of detection as compared to GCE/*o*AP and GCE/thionine controls. Preliminary results indicate that the sensors are selective to AA and can be applied to real samples.

Acknowledgments

JPB thanks the Departament d'Enginyeria Química of Universitat Rovira i Virgili for a predoctoral scholarship. Financial support from Ministerio de Economía y Competitividad, Spain (Grant BIO2012-30936 to AF), is gratefully acknowledged.

References

1. M. J. Moorcroft, J. Davis, R. G. Compton, Talanta, 54 (2001) 785-803.
2. K. Matsumoto, K. Yamada, Y. Osajima, Anal. Chem. 53 (1981) 1974-1979.
3. A. M. Pisoschi, A. F. Danet, S. Kalinowski, J. Autom. Methods. Manag. Chem. 2008, (2008) 937651. DOI: 10.1155/2008/937651.
4. A. Kannan, A. Sivanesan, G. Kalaivani, A. Manivel, R. Sevvel, RSC Adv. 6 (2016) 96898-96907. DOI: 10.1039/C6RA18440E
5. A. F. Cheng, C. W. Tsang, Food Addit. Contam. 15 (1998) 753-758.
6. G. Frenich, M. E. H. Torres , A. B. Vega , J. L. M. Vidal , P. P. Bolaños, J. Agric. Food. Chem. 53 (2005) 7371-7376.
7. K. M. Phillips, M. T. Tarragó-Trani, S. E. Gebhardt , J. Exler, K. Y. Patterson, D. B. Haytowitz, P. R. Pehrsson, J. M. Holden, J. Food Comp. Anal. 23 (2010) 253-259.
8. M. Levine, S. C. Rumsey, R. Daruwala, J. B. Park, Y. Wang, JAMA 281 (1999) 1415-1423.
9. R.A. Scanlan, Cancer Res. 43 (1983) 2435s-2440s.
10. J. S. Griesenbeck, M. D. Steck, J. C. Huber, J. R. Sharkey, A. A. Rene, J. D. Brender, Nutr. J. 8 (2009) 16.
11. D. C. Siu, A. Henshall, J. Chromatogr. A 804 (1998) 157-160.
12. I. Shah, A. Petroczi, R. A. James, D. P. Naughton, J. Anal. Bioanal. Tech. S12 (2013) 003. DOI: 10.4172/2155-9872.S12-003
13. Z. Gazdik, O. Zitka, J. Petrlova , V. Adam, J. Zehnalek, A. Horna, V. Reznicek , M. Beklova, R. Kizek, Sensors 8 (2008) 7097-7112.
14. S. M. Oliveira, T. I. M. S. Lopes, A. O. S. S. Rangel, J. Food Sci. 69 (2004) C690–C695.

15. V. H. Sastry, R. P. Moudgal, J. Mohan., J. S. Tyagi, G. S. Rao, Anal. Biochem. 306 (2002) 79-82.

16. a) H. Yang, J. Irudayaraj, J. Pharm. Pharmacol. 54 (2002) 1247-1255. b) T. Moeslinger, M. Brunner, I. Volf, P. G. Spieckermann, Clin. Chem, 41 (1995) 1177-1181.

17. M. Badea, A. Amine, M. Benzine, A. Curulli, D. Moscone, A. Lupu, G. Volpe, G. Palleschi, Microchim. Acta 147 (2004) 51-58. DOI: 10.1007/s00604-004-0220-8.

18. H. Karimi-Maleh, M. Moazampour, M. Yoosefian, A. L. Sanati, F. Tahernejad-Javazmi, M. Mahani, Food Anal. Meth. 7 (2014) 2169-2176.

19. A. Amine, M. Badea, G. Palleschi, D. Moscone, G. Volpe, A. Curulli, J. Electroanal. Chem. 509 (2001) 66-72.

20. W. Okiei, M. Ogunlesi, L. Azeez, V. Obakachi, M. Osunsanmi, G. Nkenchor, Int. J. Electrochem. Sci. 4 (2009) 276-287. No DOI available.

21. S. Skrovankova, J. Mlcek, J. Sochor, M. Baron, J. Kynicky, T. Jurikova, Int. J. Electrochem. Sci. 10 (2015) 2421-2431. No DOI available.

22. L. Civit. H. M. Nassef, A. Fragoso, C. K. O'Sullivan, J. Agric. Food. Chem. 56 (2008) 10452-10455.

23. B. Florou, M. I. Prodromidis, M. I. Karayannis, S. M. Tzouwara-Karayanni, Anal. Chim. Acta 409 (2000) 113-121.

24. a) G. Zeng, Y. Zhu, Y. Zhang, C. Zhang, L. Tang, P. Guo, L. Zhang, Y. Yuan, M. Cheng, C. Yang, Environ. Sci.: Nano, 3 (2016) 1504 -1509; b) Y. Zhu, G. Zeng, Y. Zhang, L. Tang, J. Chen, M. Cheng, L. Zhang, L. He, Y. Guo, X. He, M. Lai, Y. He, Analyst 139 (2014) 5014-5020; c) Y. Zhang, G.M. Zeng, L. Tang, J. Chen, Y. Zhu, X.X. He, Anal. Chem. 87 (2015) 989–996.

25. a) K. Lin, P. Yeh, S. Chen, Int. J. Electrochem. Sci. 7 (2012) 12752-12763. No DOI available. b) K. S. Ngai, W. T. Tan, Z. Zainal, R. M. Zawawi, M. Zidan, Int. J. Electrochem. Sci. 8 (2013) 10557-10567. No DOI available.
26. M. Nithya, J. Biosens. Bioelectron. 6 (2015) 1. DOI: 10.4172/2155-6210.1000164
27. B. R. Kozub, N. V. Rees, R. G. Compton, Sens. Actuators B 143 (2010) 539-546.
28. K. Zhao, H. Song, S. Zhuang, L. Dai, P. He, Y. Fang, Electrochem. Commun. 9 (2007) 65-70.
29. A. Bijad, H. Karimi-Maleh, M. A. Khalilzadeh, Food Anal. Meth. 6 (2013) 1639–1647. DOI: 10.1007/s12161-013-9585-9
30. L. Jiang, R. Wang, X. Li, L. Jiang, G. Lu, Electrochem. Commun. 7 (2005) 597.
31. N. Zhu, Q. Xu, S. Li, H. Gao, Electrochem. Commun. 11 (2009) 2308-2311.
32. L. H. Chen, J. B. Zang, Y. H. Wang, L. Y. Bian, Electrochim. Acta 53 (2008) 3442-3445.
33. D. Ugarte, Nature 359 (1992) 707-709.
34. J. Bartelmess, S. Giordani, Beilstein J. Nanotechnol. 5 (2014) 1980-1998. DOI: 10.3762/bjnano.5.207
35. J. P. Bartolome, L. Echegoyen, A. Fragoso, Anal. Chem. 87 (2015) 6744-6751.
36. J. Breczko, M.E. Plonska-Brzezinska, L. Echegoyen, Electrochim. Acta 72 (2012) 61-67.
37. M. Delamar, R. Hitmi, J. Pinson, J. M. Saveant, J. Amer. Chem. Soc. 114 (1992) 5883-5884.
38. S. Baranton, D. Belanger, J. Phys. Chem. B 109 (2005) 24401-24410.
39. R. Polsky, J. C. Harper, D. R. Wheeler, S. M. Dirk, D. C. Arango, S. M. Brozik, Biosens. Bioelectron. 23 (2008) 757-764.

40. A. Kowalczyk, A. Nowicka, R. Jurczakowski, M. Fau, A. Krolikowska, Z. Stojek, Biosens. Bioelectron. 26 (2011) 2506-2512.
41. H. M. Nassef, A. Radi, C. K. O'Sullivan, Anal. Chim. Acta 583 (2007) 182-189.
42. H. M. Nassef, A. Radi, C. K. O'Sullivan, Electrochem. Commun. 8 (2006) 1719-1725.
43. H. M. Nassef, L. Civit, A. Fragoso, C. K. O'Sullivan, Analyst 133 (2008) 1736-1741.
44. C. Deng, J. Chen, Z. Nie, M. Yang, S. Si, Thin Solid Films 520 (2012) 7026-7029.
45. Q. Li, J. Zhang, H. Yan, M. He, Z. Liu, Carbon, 42 (2004) 287-291.
46. A. Salimi, A. Noorbakhsh, S. Soltania, Electroanalysis 18 (2006) 703-711.
47. L. Meng, P. Wu, G. Chen, C. Cai, Y. Sun, Z. Yuan, Biosens. Bioelectron. 24 (2009) 1751-1756.

Table 1. Analytical parameters of the developed sensors and comparison with other methods.

Surface or method	Analyte	LOD (μM)	Sensitivity (μA/μM)	Linear range (μM)	Reference
GCE/CNO/*o*AP, amperometry	AA	0.34	0.024	0-50	This work
GCE/CNO/thionine, amperometry	AA	0.66	0.043	0-50	This work
GCE/*o*AP, amperometry	AA	0.3	0.012	2-20	41
SPCE/*o*AP[†], amperometry	AA	0.86	0.032	2-20	22
Spectrophotometry, enzymatic oxidation	AA	< 0.5	-	0-1000	16b
GCE/CNO/*o*AP, amperometry	nitrite	0.82	0.034	0-50	This work
GCE/CNO/thionine, amperometry	nitrite	1.89	0.045	0-50	This work
Spectrophotometry, Griess reaction	nitrite	1	-	0-10	14

[†] Screen-printed carbon electrode

Table 2. Recovery of AA in the presence of some interferents at GCE/CNO/*o*AP electrodes.

AA concentration (μM)			
Additive	**Added**	**Found**	**Recovery of AA (%)**
Glucose (1 mM)	10.0	9.8	98
Citric acid (0.1 mM)	10.0	10.6	106

Table 3. Determination of the content of AA in a commercial orange juice at GCE/CNO/*o*AP electrodes.

Sample	Nominal contents[†]	With GCE/CNO/oAP sensor[†]	Using reference method[†]	Added (μM)	Found (μM)	Recovery of AA (%)
Orange juice	40	34 ± 2	31.5 ± 0.6	10.0	10.4	104

[†] In mg/100 mL

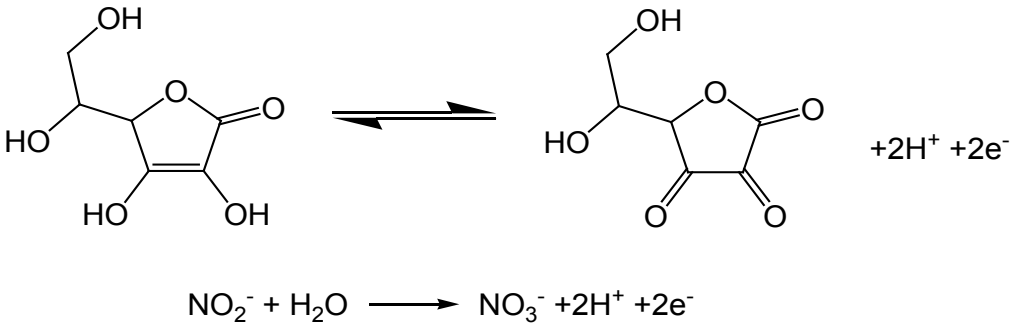

$NO_2^- + H_2O \longrightarrow NO_3^- + 2H^+ + 2e^-$

Scheme 1

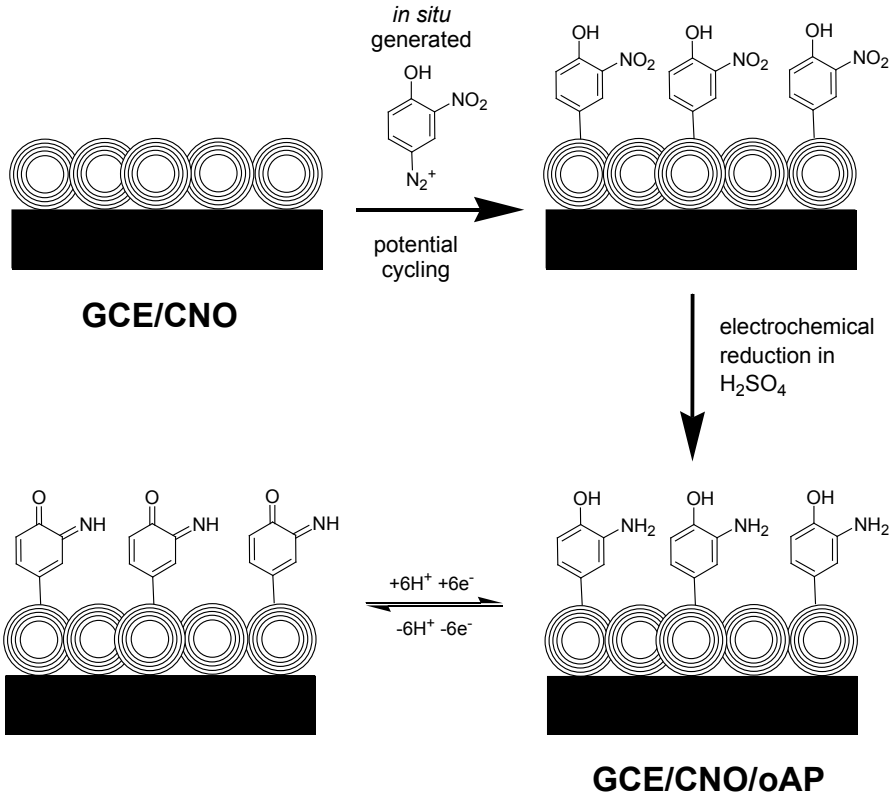
in situ
generated
OH
NO2
N2+
potential
cycling
GCE/CNO
electrochemical
reduction in
H2SO4
+6H+ +6e-
-6H+ -6e-
GCE/CNO/oAP

Scheme 2

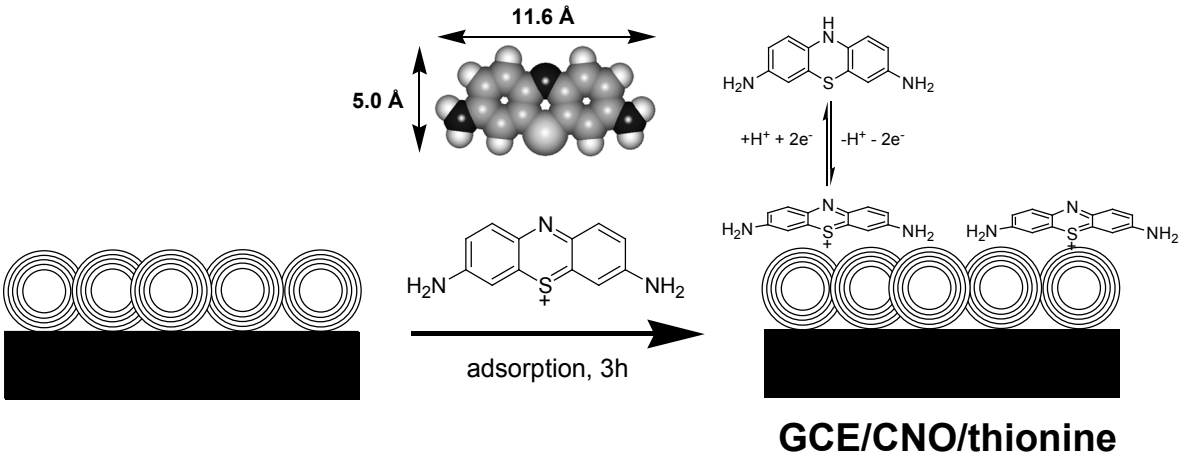

Scheme 3

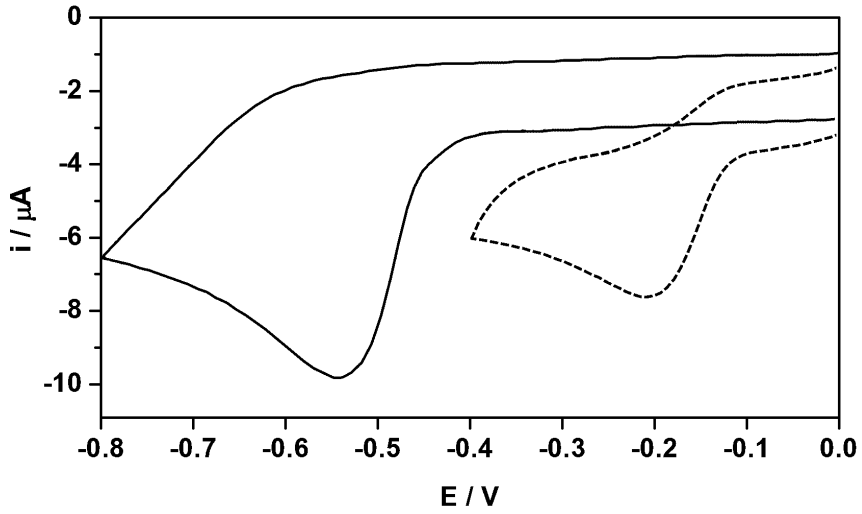

Figure 1. Cyclic voltammograms on GCE/CNO (first cycle) corresponding to the electrodeposition of 2-nitro-4-diazophenol salt in 0.5 M HCl (dotted line) and reduction of the corresponding 2-nitrophenol film in 1 M H_2SO_4. Scan rate: 100 mV/s.

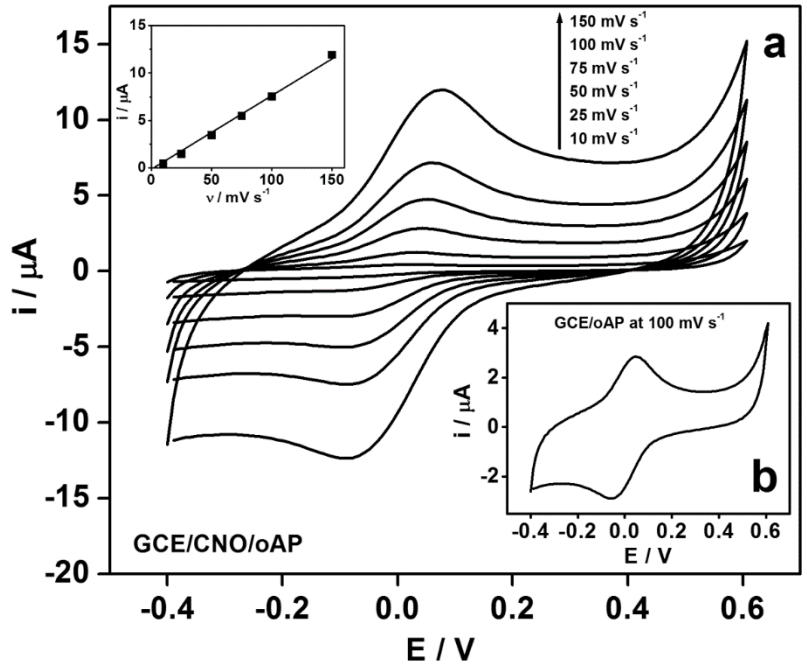

Figure 2. Cyclic voltammograms at different scan rates of electrografted *o*AP on GCE/CNO (a) and GCE (b) in phosphate citrate buffer pH 3.5.

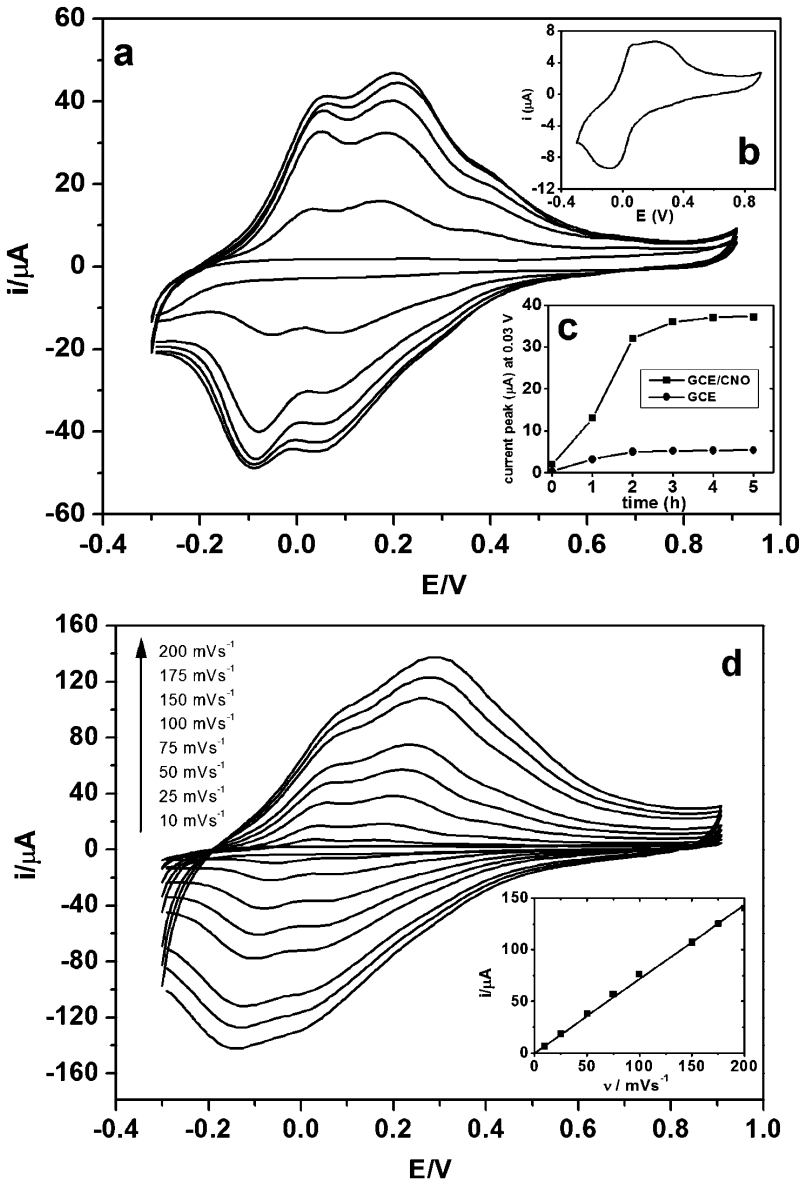

Figure 3. a) Cyclic voltammograms of thionine at different incubation times (0, 1, 2, 3, 4, 5 h) on GCE/CNO. (b) Cyclic voltammogram of thionine at bare GCE after 3 h of incubation. c) Dependence of the anodic current signal at 0.03 V with time for both surfaces. Scan rate: 50 mVs^{-1} in phosphate citrate buffer pH 3.5. d) Cyclic voltammograms of adsorbed thionine in GCE/CNO at different scan rates in phosphate citrate buffer pH 3. Inset: current vs. scan rate plot.

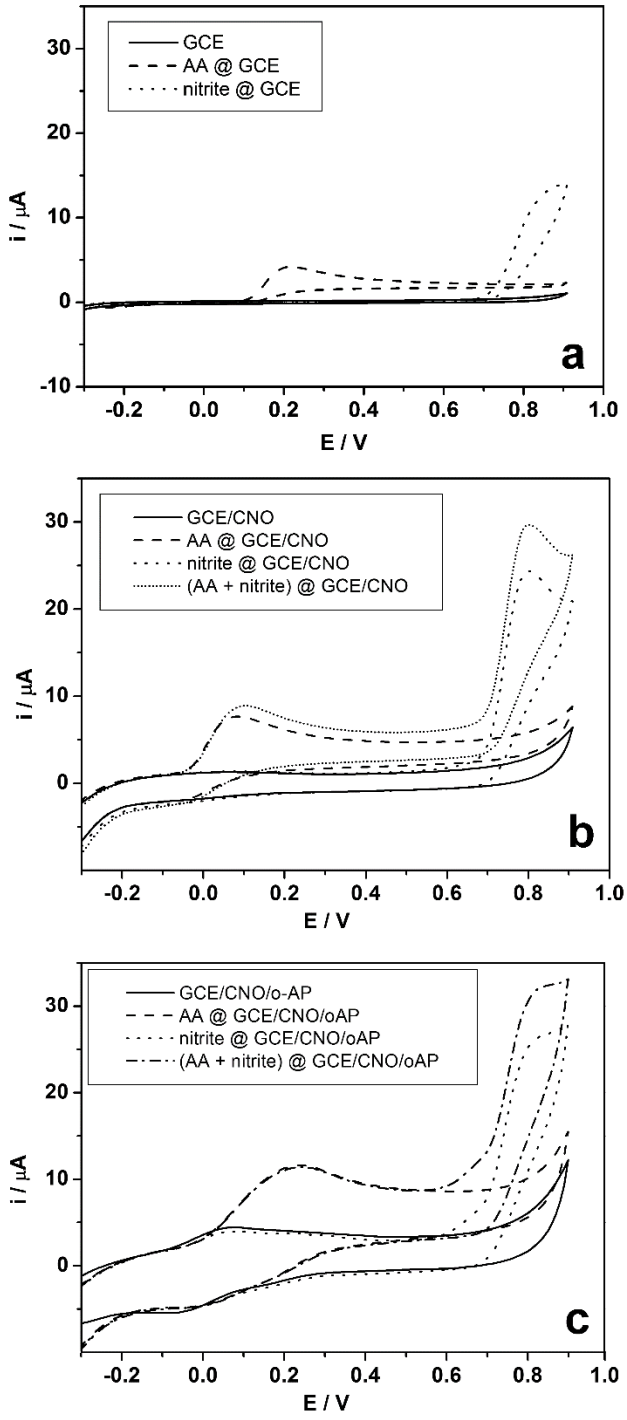

Figure 4. Cyclic voltammograms at GCE (a), GCE/CNO (b) and GCE/CNO/*o*AP (c) in the presence of 10 μM nitrite, 10 μM AA or a mixture of both (10 μM each). Scan rate 100 mV/s phosphate citrate buffer pH 3.5.

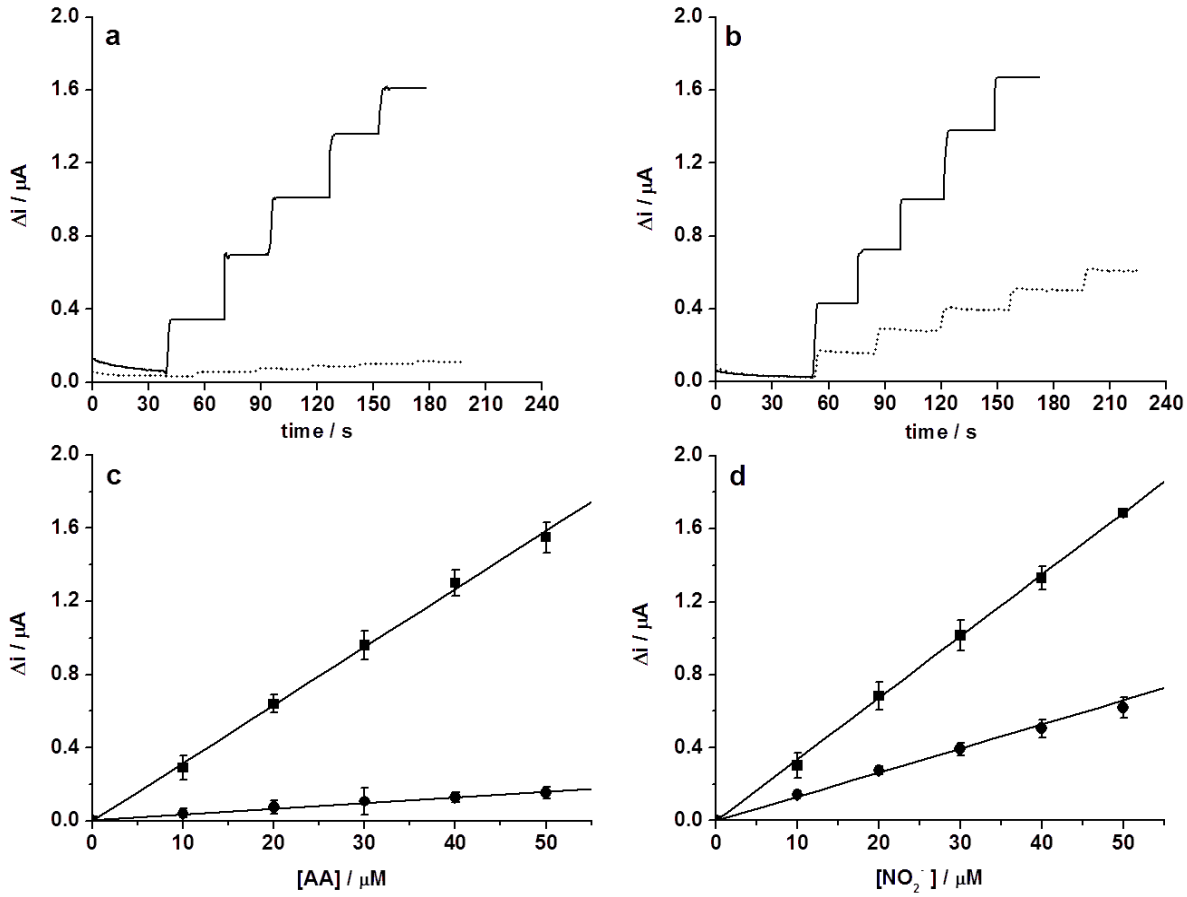

Figure 5. Amperometric responses at GCE/CNO/*o*AP (—, ■) and GCE/*o*AP (·····,●) for: (a) addition of 10 μM AA in the presence of 10 μM nitrite at +200 mV; (b) the successive addition of 10 μM of nitrite in the presence of 10 μM AA at +750 mV; (c) and (d) corresponding calibration curves. The same modified electrodes were used in both cases for the detection of nitrite and ascorbic acid.

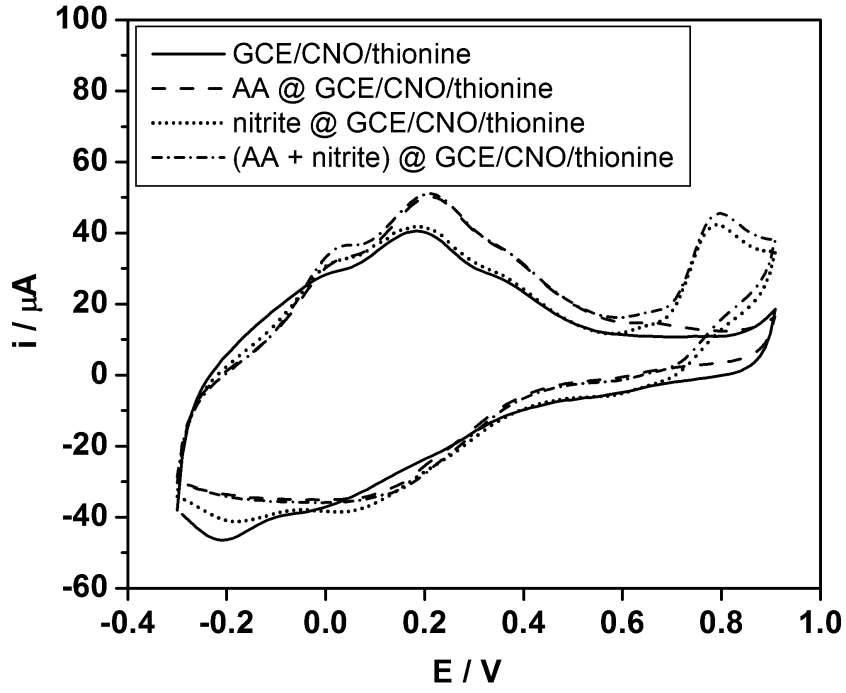

Figure 6. Cyclic voltammograms at GCE/CNO/thionine in the presence of 100 μM nitrite, 100 μM AA and a mixture of both (100 μM each). Scan rate 100 mV/s in phosphate citrate buffer pH 3.5.

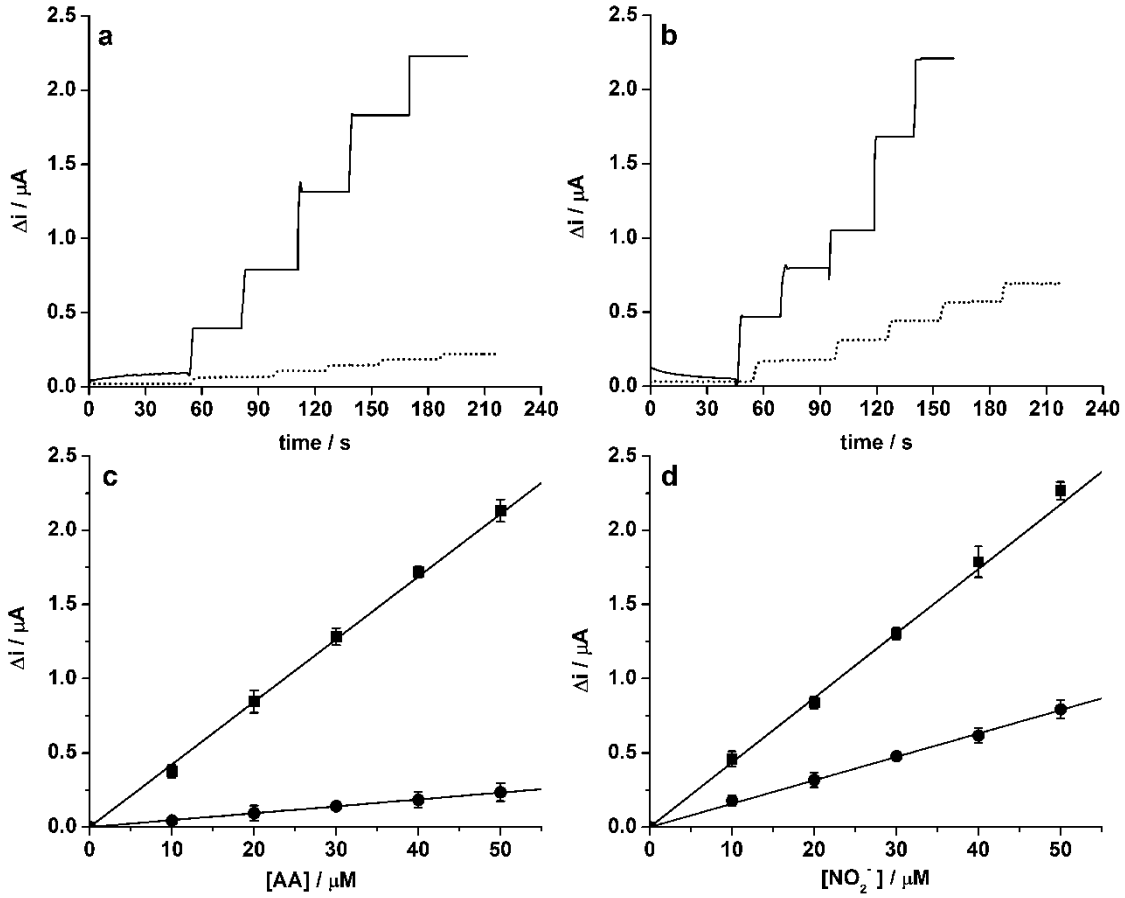

Figure 7. Amperometric responses at GCE/CNO/thionine (—, ■) and GCE/thionine (·····,●) for: (a) addition of 10 μM AA in the presence of 10 μM nitrite at +200 mV; (b) the successive addition of 10 μM of nitrite in the presence of 10 μM AA at +750 mV; (c) and (d) corresponding calibration curves. The same modified electrodes were used in both cases for the detection of nitrite and ascorbic acid.

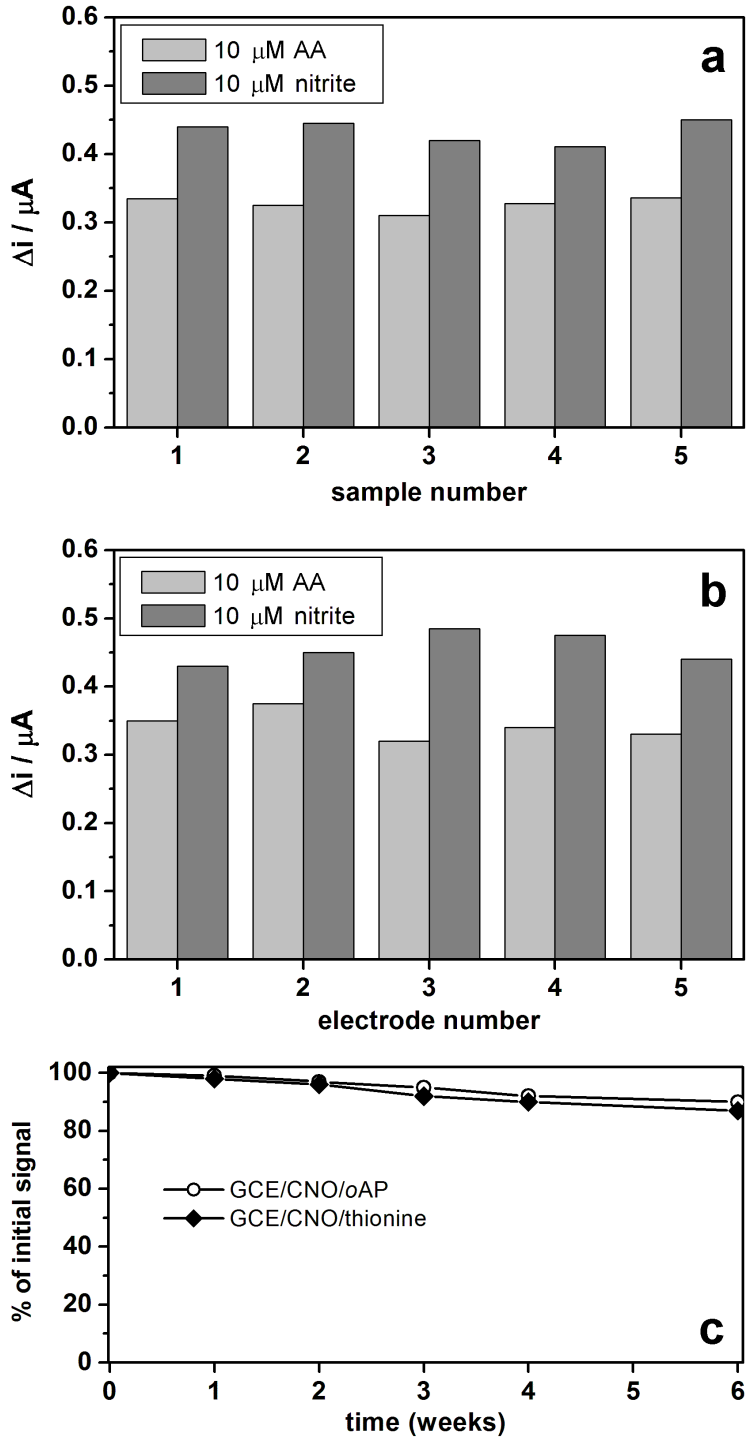

Figure 8. Amperometric responses obtained for the detection of 10 μM nitrite and AA in five different test samples (a) and five different electrodes (b) at GCE/CNO/*o*AP. (c) Stability of the sensors stored dried at 4ºC measured as the % of initial signal over 6 weeks.